Surface wetting kinetics of water soluble organic film

Majerczak, Katarzyna; Manning, Joseph R.h.; Shi, Zhiwei; Zhang, Zhanping; Zhang, Zhenyu Jason

DOI:
10.1016/j.porgcoat.2023.107436

Document Version
Publisher's PDF, also known as Version of record

Citation for published version (Harvard):
Majerczak, K, Manning, JRH, Shi, Z, Zhang, Z & Zhang, ZJ 2023, 'Surface wetting kinetics of water soluble organic film', *Progress in Organic Coatings*, vol. 177, 107436. https://doi.org/10.1016/j.porgcoat.2023.107436

Progress in Organic Coatings 177 (2023) 107436

Contents lists available at ScienceDirect

Progress in Organic Coatings

journal homepage: www.elsevier.com/locate/porgcoat

Surface wetting kinetics of water soluble organic film

Katarzyna Majerczak [a], Joseph R.H. Manning [b], Zhiwei Shi [c], Zhanping Zhang [c], Zhenyu Jason Zhang [a,*]

[a] School of Chemical Engineering, University of Birmingham, Edgbaston, Birmingham, United Kingdom B15 2TT
[b] Department of Chemical Engineering, University of Manchester, Manchester, United Kingdom M13 9PL
[c] The Procter and Gamble Company, Mason Business Center, 8700 Mason Montgomery Road, Mason, OH 45040, United States

ARTICLE INFO

Keywords:
Wetting kinetics
Water soluble
Contact angle
AFM

ABSTRACT

The wetting kinetics of poly(vinyl alcohol) (PVA)-based films by water was investigated using contact angle (CA) goniometry, Fourier-transform infrared spectroscopy, and atomic force microscopy. We show that CA evolution is determined by four main factors: film composition, preparation method, presence of plasticiser in the matrix, and relative humidity (RH) conditions during aging. All formulations prepared from partially hydrolysed polymer were less susceptible to dissolution compared to fully hydrolysed counterparts, with the CA evolution character shifting from exponential to linear for respective formulations. This behaviour is likely attributed to the intrinsic properties of PVA matrices, i.e. changes in free volume, tortuosity, as well as size and distribution of crystalline regions. Incorporation of glycerol as a plasticiser results in overall faster CA evolution, with surface spreading playing more significant role compared to non-plasticised samples. Furthermore, aging of PVA-based films does not lead to profound changes in any environment except 100% RH. For these conditions, the initial stages of PVA dissolution due to water absorption were observed, with the changes in the matrix continuity dependent on PVA degree of hydrolysis. These results expand on the understanding of initial stages of polymer dissolution in consumer goods products and can pave the way to enhanced performance and prolonged shelf life of the products.

1. Introduction

Poly(vinyl alcohol) (PVA) is a polymer that exhibits a range of industrially desirable properties, including good film forming capability [1,2], low toxicity [3], and water-solubility [4]. However, other intrinsic properties of pure PVA such as brittleness and low flexibility [5] need to be improved prior to its application in finished products, e.g. by controlling the degree of hydrolysis (DH) and molecular weight (M_w). More significant changes are often introduced to meet industrial requirements, resulting in formulated products consisting of PVA and several performance-enhancing additives (e.g. plasticisers) [6]. While the mechanical properties are improved, the presence of additives results in changes in polymer matrix structure and intermolecular interactions, with potentially detrimental effects to the resultant product quality. Accordingly, understanding the effect of formulation composition on PVA behaviour is crucial for developing improved consumer products.

Regardless of DH, M_w, and presence of additives, PVA displays a semicrystalline nature with small crystalline domains embedded in the amorphous phase [7]. In general, introducing plasticisers to the system (e.g. glycerol [8,9], propylene glycol [10], ethanolamines [11], or water [12]) leads to a decrease in overall degree of crystallinity (DC) in the polymer matrix. Water plays an additional role in the system, acting as a solvent in sufficiently high concentrations. Due to the hydrophilic nature of PVA, polymer powder contains ca. 6.5 wt% water at ambient temperature [13] before any processing, which increases with increasing relative humidity (RH). Below a threshold concentration of ca. 22 wt% [14], water is present within PVA films in a nonfreezing state, although this limit may be increased by the presence of additives with high affinity to the polymer chain or changes to the polymer DH [15]. After exceeding this threshold, water becomes mobile within the matrix and begins to disrupt the intermolecular hydrogen bond network between amorphous and crystalline PVA regions [14]. As water is not present in the region of intact crystallites, the total amount of water in the system is equal to water content in the polymer amorphous region [14]. Consequently, overall DC is an important factor when considering

* Corresponding author.
E-mail address: z.j.zhang@bham.ac.uk (Z.J. Zhang).

https://doi.org/10.1016/j.porgcoat.2023.107436
Received 23 October 2022; Received in revised form 13 January 2023; Accepted 15 January 2023
Available online 3 February 2023

dissolution of PVA by water.

Polymer wetting is a crucial step during the manufacturing process of PVA-based formulations, e.g. single-dose laundry pods, where during their assembly a thin water layer is distributed on two PVA-based films followed by pressing together. The wetting process leads to partial film dissolution, enabling interdiffusion of polymer chains hence sealing the pouch. Understanding water wetting phenomenon of water-soluble films can therefore enable tuning of the PVA-based formulations, improving control over product performance both during manufacture and at later stages in the supply chain.

Wetting behaviour of PVA-based formulations has been studied in humid air to investigate water sorption in polymer materials in the presence [16–18] and absence [19] of additives. Moreover, changes in the structure of PVA formulations (i.e. swelling) upon contact with various liquids [20–23] as well as solvent (i.e. water [2,5,24] and acetone [24]) migration in pure [2] and modified polymer matrices with fillers [24] and plasticisers [5] was tackled. These studies highlight the importance of the system chemical composition on its overall behaviour, albeit providing inconsistent conclusions for the same system [2,24]. Additionally, despite the diversity of systems studied, no information pertaining to the initial polymer/solvent contact can be concluded due to the limitations of the experimental techniques used (e.g. FTIR and Raman spectroscopy, or swelling tests), while the short time scale associated with the sealing process generates a need to understand polymer wetting mechanism immediately upon contact with a liquid medium.

By contrast, contact angle (CA) goniometry combined with high-speed cameras is a promising technique to capture the initial wetting kinetics on polymer films. Generally understood as a constant value, contact angle for materials soluble in the medium (here - hydrophilic PVA soluble in water) naturally changes over time until an equilibrium is achieved. CA measurements provide information about evolution of contact angle, allowing study of the wetting mechanism – droplet formation, spreading, and absorption (liquid movement in x,y- and z-direction, respectively) into the system [25,26] as well as changes in wetting upon aging under various RH conditions [27].

This work aims to understand how changes in the film composition (M_w and DH of PVA, addition of plasticiser, change in the storage RH) influence the wetting mechanism of PVA-based films of various thickness (spin-coated films of thickness below 250 nm and solution cast films of thickness above 10 μm). Changes in thickness, together with mathematical modelling, will help to gain insight into the main mechanism of CA evolution – spreading or absorption. First, evaluation of changes in film morphology with changes in polymer DH and film thickness are presented using atomic force microscopy (AFM) measurements. Then, the influence of system chemistry (film composition, changes in RH) on wetting behaviour is discussed for both thin and thick films using CA goniometry. Finally, FTIR measurements are presented to establish the influence of crystallinity on the polymer wetting behaviour.

2. Materials and methods

2.1. Materials

PVA (Sigma-Aldrich P8136, M_w = 30–70 kg•mol^{-1}, DH = 87 %–90 % denoted as 87PVA and Sigma-Aldrich 341584, M_w = 89–98 kg•mol^{-1}, DH = 99 %+ denoted as 99PVA), glycerol (Sigma-Aldrich G9012, ≥99.5 %), silica gel (Fisher Scientific S/0762/53, HPLC grade), potassium carbonate (Fisher Scientific P/4080/60, extra pure), and HPLC water (HPLC Plus, Sigma Aldrich 34,877-M) were purchased and used as received.

2.2. Sample preparation

PVA powder was dissolved in HPLC water by heating up to 75 °C (87PVA) or 100 °C (99PVA) with continuous stirring (for ca. 2 h or until completely dissolved) to obtain a concentration of 4 % or 10 % (w/v), and subsequently cooled to room temperature. Solutions of plasticiser (glycerol) of 4 % (w/v) were prepared by dissolving required amount of substance and stirring at room temperature for ca. 4 h. Polymer/plasticiser solutions were prepared either by mixing the respective 4 % (w/v) stock solutions or by adding pure glycerol to 10 % (w/v) to PVA solutions such that PVA/glycerol (w/w) ratio was 4:1.

Thin PVA films (<250 nm) were prepared from 4 % (w/v) solutions (both with and without glycerol) by spin coating 320 μl or 1200 μl of the solution with a spin speed of 2000 rpm for 100 s or 1000 rpm for 300 s, respectively, to obtain film of various thicknesses using a spin coater (Spin 150i, SPS-Europe). 1 in. squared glass slides were used as substrates and cleaned using piranha solution (mixture of 98 % concentrated sulphuric acid and 30 % hydrogen peroxide at a volumetric ratio of 7:3) for 1 h to remove any organic impurities [28], followed by sonication (three times, 10 min each sonication) in ultrapure deionized water (Mili-Q, 18.2 mΩ cm) and dried in an oven at 70 °C. Solution cast films (>10 μm) were prepared by placing 400 μl or 800 μl of either 4 % (w/v) or 10 % (w/v) solutions (with or without plasticiser) onto a glass slide and placing in a vacuum oven (75 °C, ca. 200 mbar) for ca. 1 h.

2.3. Experimental procedure

CA measurements were performed using a Theta Optical Tensiometer (Biolin Scientific) with an automated dispenser. To investigate the initial stages of CA evolution, measurements were performed for 90 s (RH ≈ 45 % RH, T = 19 °C), with image recording at 72 fps. HPLC water was used as testing liquid. The images illustrating CA evolution on PVA-based film over time were presented in Table S1 (Supporting Information). Every measurement was preceded by camera calibration followed by positioning the syringe 0.6 cm away above the PVA film surface. Films of each kind were prepared in triplicate. Due to the proven dependence of CA evolution on the proximity of the substrate edge [29] as well as the time difference between drop formation and deposition [30], three measurements were performed in a triangle arrangement close to the centre of the sample avoiding contact of any drop with other, with immediate deposition after its formation. Image analysis was performed using OneAttension software to obtain CA values, area of the liquid/surface contact, height of the droplet, and baseline length. The data was analysed using Python scripts to fit the mathematical model described below, as well as to perform geometrical investigations into the CA evolution mechanism and validation calculations for the chosen model [31]. For all samples, model validation to check the assumption of the spherical dome droplet shape was performed.

The effect of RH was examined by storing freshly prepared films in a desiccator with silica gel (ca. 4 % RH), saturated solution of potassium carbonate (ca. 45 % RH) [32], or water (100 % RH) for one week prior to CA measurements.

FTIR measurements were carried out to investigate changes in DC against changes in the polymer matrix microstructure within solution cast PVA-based films only. The measurements were performed on a Bruker Lumos FTIR Microscope. Spectra were recorded from 4000 to 600 cm^{-1} with 32 scans and resolution of 4 cm^{-1} using diamond as ATR-FTIR crystal (penetration depth of ca. 2 μm). Measurements lasted for <5 min, preventing films from changing in response to ambient RH. Baseline data correction was performed using airPLS algorithm [33] applied in Python scripts. Crystallinity was determined using ratio of the intensity of the crystalline to non-crystalline peaks as described in the literature [7,34–38].

AFM was used to observe changes to surface morphology with composition (both spin-coated and solution cast), and to measure film thickness (for spin-coated films). Imaging in tapping mode utilised tapping mode cantilevers (μmasch, HQ:NSC15/AL BS, aluminium coating, spring constant of ca. 40 N/m) and was performed on a Dimension 3100 AFM (Veeco). Scratch test for thickness measurements was performed by applying potential difference equal to 14 V with

scanning angle equal to 0°, followed by imaging at the scanning angle equal to 90° [39]. For each sample, three scratches were made and at least three depth profiles from each scratch were extracted. The sample thickness was taken as the average value from all analysed positions. Thickness of solution cast films was determined using a digital micrometer.

3. Results and discussion

3.1. Model validation

CA evolution over time is a consequence of the liquid/solid/air interactions which can be deconvoluted into two key phenomena - spreading and absorption. Spreading arises due to variations in energy states of the solid surface, its adsorption behaviour and wetting kinetics, which can be correlated to the droplet shape and structure of the surface. It can be either direct (through flux of liquid water in contact with the film) or indirect (through evaporation of water from the droplet and subsequent condensation ahead of the contact line) [40]. Conversely, absorption is primarily determined by the surface structure of the solid [25], its porosity, and free volume. In the case of PVA-based formulations, the hydrophilic nature of the polymer, its dissolution in water and changes in free volume of the material all contribute to absorption.

To account for the concurrent absorption and spreading observed in water-soluble polymers [31], Farris et al. developed a model using semi-empirical exponential decay akin to the Avrami mechanism of crystallisation kinetics [41], or equations used to establish the length of a capillary [42,43]. The equation takes the following form:

$$\theta(t) = \theta(0)\cdot e^{kt^n} \tag{1}$$

where θ(t) and θ(0) are the contact angles at a given time t and time 0, respectively, k is the rate of contact angle evolution, and n is linked to physicochemical phenomena underlying the overall process, describing the fractional values normally attributed to the presence of two or more phenomena that occur simultaneously. Theoretically, $n = 0$ in the case of pure absorption (a constant CA value) and $n = 1$ in the case of pure spreading (exponential decrease in CA value). To corroborate the mechanism implied by the value of n, geometrical analysis of the solvent droplet below can be used:

$$\Delta S_B = (\Delta S_B)_{absorption} + (\Delta S_B)_{spreading} \tag{2}$$

$$(\Delta S_B)_{absorption} = 3\left[\frac{(V - V_0)}{h}\cdot\left(\frac{1 + cos\theta}{2 + cos\theta}\right)\right] \tag{3}$$

$$(\Delta S_B)_{spreading} = 3V_0\left[\frac{1}{h}\left(\frac{1 + cos\theta}{2 + cos\theta}\right) - \frac{1}{h_0}\cdot\left(\frac{1 + cos\theta}{2 + cos\theta}\right)\right] \tag{4}$$

where V, V_0, h, and h_0 are the volume and height of the droplet at time t and 0, respectively, and ΔS_B is the area of liquid-solid contact (the basal area). To conclude which phenomenon is predominant, all ΔS_B values were normalised against the initial area, S_{B0}. Although this model assumes a perfect spherical droplet shape, the combined approach enables validation of this assumption. Because of the additional geometrical check of the dominating wetting mechanism in the system, the model by Farris et al. is more relevant for the investigations presented here than models previously described in literature [25,26,29,44–49] and was used to establish kinetics of water migration in PVA-based systems.

To confirm the other assumptions of the Farris model are appropriate for this study, i.e. that the effects of gravity and evaporation are negligible, the following equation was used: [50]

$$l_0 < \left(\frac{2\gamma_{lv}}{\rho g}\right)^{0.5} \tag{5}$$

where l_0 is lineal dimension of the droplet, ρ is the density of the liquid, and g the gravitational acceleration. Given l_0 was smaller than the right-hand side of Eq. (5) (here found to be ca. 3.5 mm and 3.8 mm respectively, at t = 0), it was determined that gravity can be neglected. Similarly, to confirm that evaporation does not play a significant role, preliminary measurements on pure glass substrates were performed finding no significant change to droplet volume over the length of the experiment. Together with the short measurement duration (<90 s cf. several minutes for experiments where evaporation plays an important role) [27], these results confirm that evaporation is negligible.

3.2. PVA film surface characteristics

Spin coating is based on rapid solvent evaporation, leading to formation of thin films with non-equilibrium structure. For solution-casting, however, elevated temperature and prolonged evaporation time allow the sample to reach an energetically favourable structure. The differences in preparation method might result in variations in surface roughness, in turn influencing wetting kinetics [51,52]. PVA films studied here showed a uniform morphology (Fig. 1) and low roughness (maximum of ca. 1 nm, Table 1). In general, 99PVA films had an increased roughness, though the difference was negligible. Therefore, it can be concluded that surface roughness is not responsible for any potential differences in water migration kinetics observed between the two preparation methods.

Due to the higher M_w of 99PVA, films of these polymer were ca. 38 % thicker than corresponding 87PVA formulations (Table 1). Introducing chosen glycerol content (20 wt%) to PVA system was proven to lead to sufficiently flexible films without causing significant changes in film thickness [5]. Here, the addition of glycerol typically did not decrease the film thickness by >20 %. The most notable differences were observed for solution cast films prepared from mixed 4 wt% polymer and plasticiser solutions, while a difference of only max. 6 % was observed for thin films prepared using 1000 rpm spin speed (Table 1).

3.3. Effect of composition change on water spreading behaviour for thin films

Thin films prepared from PVA of various DH exhibited distinct features in the CA evolution (Fig. 2a). For non-plasticised 87PVA (Fig. 2a, black and grey lines), an initial exponential decrease was observed. For 99PVA, the trend appears almost as a linear decrease (Fig. 2a, red and orange lines), which is similar to that of hydrophobic materials, on which the CA changes are caused solely by evaporation (in prolonged experiments) [53]. Generally, the thinner the film, the quicker the CA evolved. However, because the character of CA evolution did not change with the film thickness for any of the investigated DH, the differences in CA evolution between 87PVA and 99PVA cannot be attributed to differences in film thickness alone; they result from the intrinsic properties of the matrix.

Spreading is a much faster process compared to absorption due to the necessity of solvating polymer chains in the latter case [24]. Hence, the initial CA evolution is likely correlated with spreading, followed by infiltration. From geometrical analysis of water droplets (Eqs. (2)–(4)), 87PVA showed greater spreading than absorption (Fig. 2b). For 99PVA, however, spreading had a similar magnitude as absorption although both mechanisms were less prominent compared to 87PVA, echoing the trend in ΔCA for these formulations.

Despite the much-reduced spreading behaviour, 99PVA is more hydrophilic than 87PVA as evidenced by the lower initial CA (ca. 41° cf. 54°, respectively, Table 1). This may be due to the differences in hydrogen bonding behaviour of the two polymers - assuming that each water molecule binds to a hydroxyl group of PVA chains [14] before acting as a freezable water, the amount of water molecules needed for 99PVA saturation would be 2.06 times greater than that required for 87PVA (per chain, based on M_w and DH). Moreover, despite the fast solvent evaporation kinetics during spin coating, the overall DC is

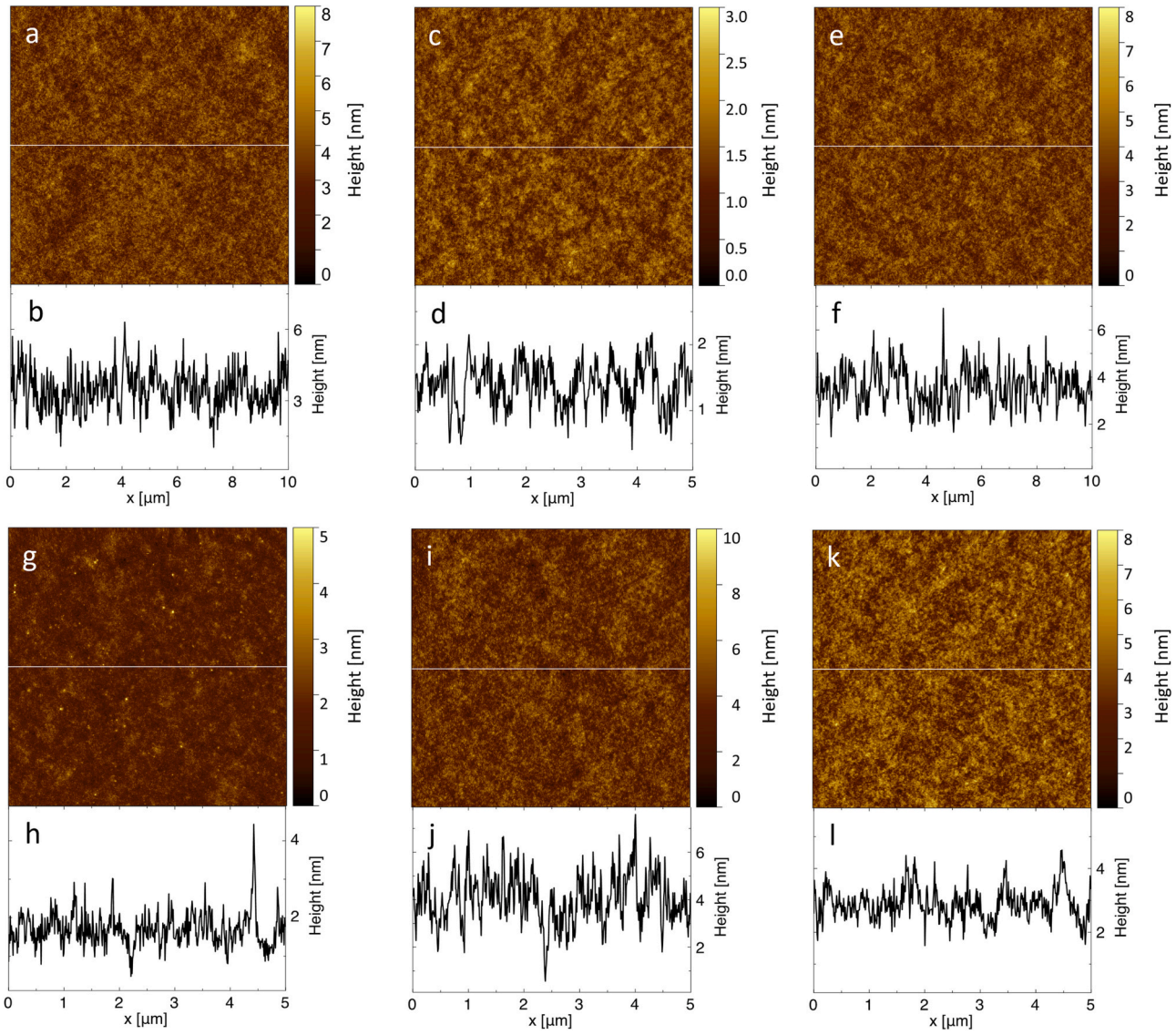

Fig. 1. Morphology and height profile of: (a, b) spin-coated plasticised 87PVA film, (c, d) solution cast 87PVA film, (e, f) solution cast plasticised 87PVA film, (g, h) spin-coated 99PVA film, (i, j) solution cast 99PVA film, and (k, l) solution cast plasticised 99PVA film.

expected to be higher for 99PVA; these crystallites are additional obstructions for migrating water.

Changes in DC were previously reported to change the dissolution mechanism of PVA thin films by controlling the polymer relaxation rate and swelling behaviour [23]. Hence, higher amount of crystallites would result in decelerated CA evolution behaviour. However, it is also probable that the difference in M_w of the two PVA types studied could affect the surface spreading and absorption [54,55]. The high M_w and DH of 99PVA result in interchain interactions which creates a matrix of higher tortuosity hence additional obstructions for water movement within the matrix. This behaviour is like that of PVA in solutions as decreased solubility is observed for polymers with higher DH or M_w, where more energy is required to disrupt the hydrogen bonding and cause dissolution.

Plasticisation of the films with glycerol markedly accelerated the CA evolution for all PVA formulations: an exponential decrease or a drastic reduction followed by linear decay was observed for 87PVA and 99PVA, respectively (Fig. 2a), resulting in both absorption and spreading components being negative at the beginning of the experiment for these compositions (Fig. 2b). This rapid kinetics of CA evolution on plasticised 99PVA films prevented meaningful image analysis as after the initial CA decrease as the droplet edges could not be reliably detected (truncated CA evolution line for 99PVA + G 124 nm, Fig. 2b).

Initial CA values for plasticised samples were, rather surprisingly, greater than those of unplasticized counterparts (ca. 61° for plasticised PVA cf. 54° for non-plasticised, Table 1), which indicates more hydrophobic surface nature for the former. For PVA of both DHs, inclusion of plasticiser also increased ΔCA over the entire duration of the measurement (Table 1). In PVA formulations, glycerol replaces PVA-PVA hydrogen bonds, accelerating disruption of hydrogen bond network and lowering water content required to reach limit of nonfreezing state - hence faster spreading and absorption.

Upon fitting the CA kinetics with the model of Farris et al. (Eq. (1), Fig. 3), the average values of n were 0.26–0.37 for 87PVA (with or without the presence of glycerol, Fig. 3b, Table S2 in Supporting Information), suggesting that spreading contributes substantially to the wetting mechanism in these samples. By contrast, samples of non-plasticised 99PVA showed n values of only 0.16–0.22, implying a predominance of absorption rather than spreading. However, plasticised 99PVA samples showed an inverse behaviour, with n values of 0.37–0.54, indicating even more spreading than any 87PVA sample (Fig. 3b and Table S2 in Supporting Information). In general, fitted

Table 1
Average thickness, roughness, and CA evolution parameters for the investigated compositions using water as the testing liquid. Symbols represent: CA_0 – initial CA, CA_e – contact angle at the end of the measurement, ΔCA – difference between CA_0 and CA_e, ΔV – change in the droplet volume, ΔA – change in the liquid/solid contact area. Shaded cells correspond to spin-coated films. Uncertainty values represent one standard deviation around the mean (n = 9).

Sample	Thickness (μm)	Roughness (nm)	CA_0 (°)	CA_e(°)	ΔCA(°)	ΔV(μL)	ΔA(mm²)
87PVA	30.6±1.9	0.6±0.1	62.5±1.6	48.7±0.6	-13.9±1.2	-0.46±0.08	1.32±073
	44.5±3.8	0.8±0.1	73.6±1.0	61.2±1.1	-12.3±1.0	-0.17±0.16	1.17±0.33
	87.0±3.3	0.8±0.1	71.7±2.7	56.2±1.9	-15.4±1.2	-0.77±0.06	2.26±0.52
	129.7±7.6	0.7 ±0.1	66.0±2.4	57.2±2.2	-8.8±0.8	-0.31±0.05	1.09±0.15
	0.093±0.003	0.3±0.1	54.3±1.1	20.0±0.5	-34.3±1.2	-0.32±0.22	12.84±0.28
	0.120±0.003	0.3±0.1	57.8±1.9	19.9±0.1	-37.9±2.0	-0.65±0.09	11.85±0.70
Plasticised 87PVA	21.7±2.7	0.9 ± 0.1	64.4±1.8	43.8±5.2	-20.6±6.9	-0.63±0.19	2.81±1.24
	39.3±5.5	0.9±0.1	64.5±1.3	39.9±5.1	24.6±5.4	-0.40±0.18	5.04±1.61
	73.5±4.5	0.8±0.1	68.3±0.6	39.5±1.0	-28.8±1.2	-0.94±0.38	5.33±1.02
	108.8±3.0	1±0.1	68.5±2.7	34.5±1.3	-34.1±3.6	-0.34±0.14	5.12±0.48
	0.078±0.001	0.3±0.1	61.7±0.6	18.5±0.3	-43.2±0.8	-0.40±0.13	14.13±0.77
	0.118±0.001	0.3±0.1	64.5±0.9	21.6±1.6	-42.9±2.0	-0.45±0.23	11.91±1.14
99PVA	52.8±2.3	1±0.1	47.4±1.1	40.5±1.2	-6.8±1.3	-0.29±0.03	0.25±0.06
	88.3±4.6	1.2±0.1	45.7±1.2	36.0±1.6	-9.7±1.2	-0.29±0.04	0.34±0.08
	129.7±3.3	0.9±0.1	50.1±2.8	41.5±1.2	-8.6±2.2	-0.35±0.07	0.33±0.13
	208.5±2.2	1.0±0.1	47.2±1.3	41.1±1.1	-6.1±1.1	-0.32±0.04	0.27±0.09
	0.149±0.009	0.4±0.1	41.6±1.0	36.4±0.6	-5.2±0.6	-0.33±0.01	0.06±0.01
	0.192±0.013	0.6±0.1	43.1±0.7	38.8±0.6	-4.3±0.3	-0.30±0.02	0.10±0.06
Plasticised 99PVA	33.1±3.3	1±0.1	39.5±1.1	27.5±0.4	-12.1±0.9	-1.12±0.24	4.16±1.43
	65.8±3.0	0.9±0.1	38.2±2.4	26.8±0.3	-11.5±2.5	-3.02±0.81	3.45±0.97
	119.8±2.1	0.9±0.1	52.8±2.7	19.6±1.2	-33.2±2.5	-0.96±0.36	13.64±2.92
	169.2±4.1	1.4±0.1	47.5±3.1	22.6±1.3	-24.9±3.7	-0.36±0.19	7.94±1.54
	0.124±0.001	0.7±0.1	52.3±0.9	22.2±2.1	-30.2±2.4	-3.22±0.86	16.27±4.67
	0.181±0.003	0.8±0.1	47.8±1.3	15.0±0.8	-32.8±1.8	-0.44±0.08	28.28±12.88

values for time constant k (Fig. 3a, Table S2 in Supporting Information) naturally mirrored the overall change in CA across the duration of the experiment for samples of the same DH (Fig. 2a, Table 1) – the higher ΔCA, the lower k values.

3.4. *Effect of composition change on water spreading behaviour for thick films*

In general, PVA films prepared by solution casting showed similar CA evolution characteristics to that of spin-coated PVA films (Fig. 5a, summarised in Fig. 3), however, with less significant changes in ΔCA for all formulations except non-plasticised 99PVA (Table 1). This observation further suggests that physico-chemical properties of the polymer matrix, such as amount of free hydroxyl sites, tortuosity, free volume, as well as possible differences in crystallite size and overall DC between the two PVA types influence these distinct changes in solvent migration. For example, the cavity radius in vacuum-dried films of 99PVA was found to be smaller than that of equivalent 87PVA (2.45 Å compared to 2.64 Å, respectively [54] cf. van der Waals radius of water, 1.7 Å [56]), signifying differences in molecular packing within each polymeric matrix.

Both plasticised PVA films showed an increased rate of CA evolution compared to non-plasticised counterparts. It is worth noting that there are discontinuities in the CA evolutions of glycerol-plasticised 99PVA films (Fig. 5a, green): in those cases, a sudden spreading event was observed. There are two possible explanations for this behaviour: first, dissolution of glycerol and PVA into the droplet changed the liquid surface tension and viscosity hence CA evolution behaviour. In thin films fewer glycerol molecules were available to dissolve, therefore, changes in adjacent to film water-based solution were insignificant. Second, glycerol was incorporated into PVA crystallites as inclusion defects, which decreased the overall DC without changing the crystallite size distribution for 87PVA (although broadening the distribution for 99PVA) [58], in turn leading to accelerated dissolution of crystal structures [53,59].

The alterations in the wetting behaviour with changes in film thickness and composition might be a result of changes in the polymer state – from glassy to rubbery – due to plasticisation of the polymer by the solvent [60]. This phenomenon can be observed as the regime change (kink) while plotting change in contact line velocity (U) vs CA. U was calculated following Dupas et al. [60] as:

$$U = \frac{\theta\gamma_l(cos\theta_e - cos\theta)}{3\eta_L ln(r)} \quad (6)$$

where γ_l is the water-air surface tension, θ_e is static wetting angle, η_L is water viscosity and r is the ratio of the droplet radius and microscopic cut-off length, with typical values ln(r) equal to 10. This was, however, not observed for any films studied here (Fig. 4). While the glass transition temperature (T_g) of vacuum-dried PVA films is equal to 65 °C and 53 °C for 98 % DH and 88 % DH, respectively [10], these values decrease upon addition of 20 wt% glycerol (by ca. 30 °C) [10] or equilibration in the ambient atmosphere (by ca. 40 °C for RH = 42 %) [62]. Therefore, it is likely that although samples were not equilibrated in ambient RH prior to measurements, all formulations are in their rubbery state due to the presence of plasticisers in the system.

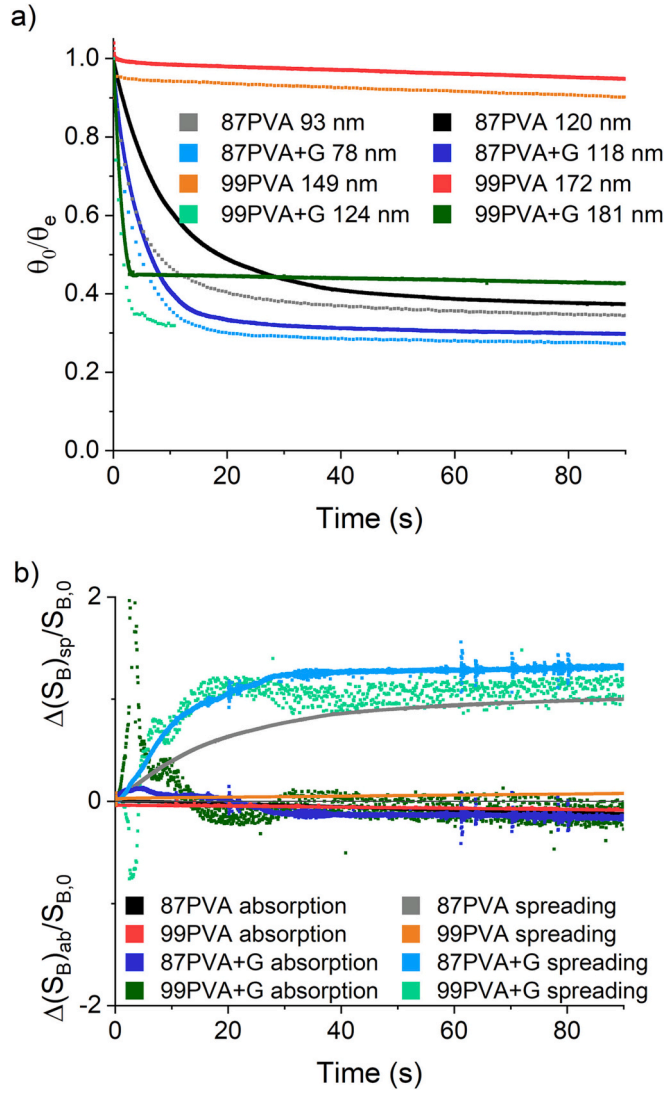

Fig. 2. (a) CA evolution for spin-coated PVA films of various composition. For clarity, formulations of lower thickness were displayed as dotted lines. (b) Corresponding geometrical investigations (Eqs. (2)–(4)) for spin-coated samples prepared using 1000 rpm spin speed. For interpretation of the references to colour in this figure, the reader is referred to the web version of this article.

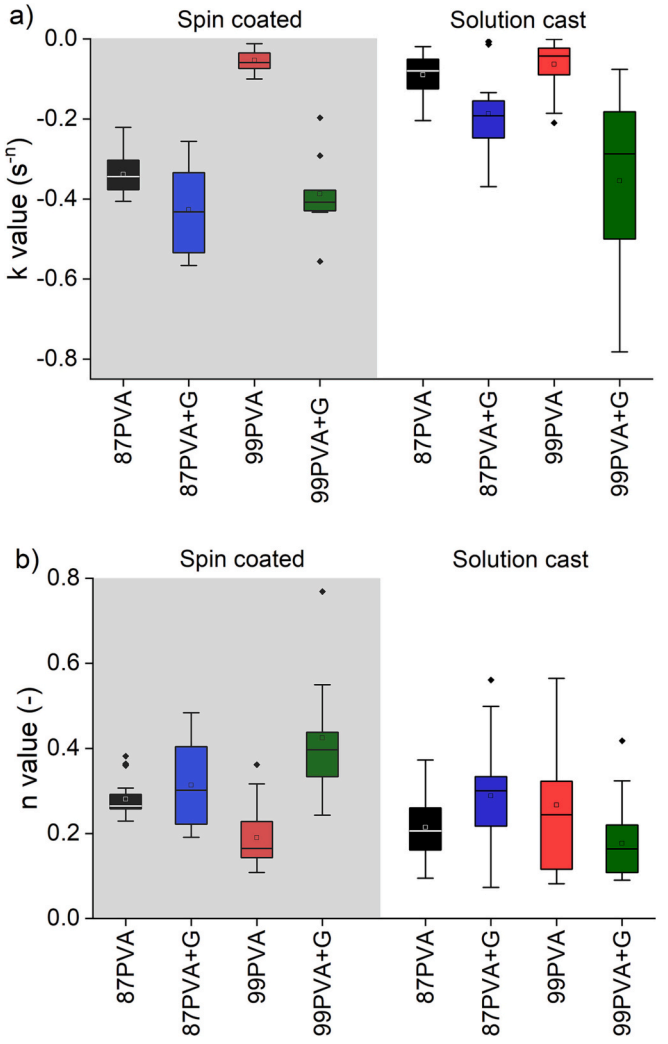

Fig. 3. Fitted values to the model by Farris et al. (Eq. (1)) for parameters (a) *k* and (b) *n* for spin-coated and solution cast films.

For formulations of 87PVA (both plasticised and non-plasticised), the evolution of U for spin-coated films is significantly accelerated compared to thicker, solution cast counterparts (Fig. 4). For non-plasticised 99PVA formulations, however, this trend was reversed, while their plasticised counterparts showed no difference in U evolution with CA between samples of different thicknesses. All results are in line with presented CA evolution with time (Figs. 2a, 5a) – the quicker CA evolution with time, the quicker U evolution with CA.

Following the geometrical analysis of the water droplet, it was concluded that spreading and absorption play similar roles to one another for non-plasticised solution cast PVA films (Fig. 5b), with fast initial CA changes leading to a steady linear increase in both factors (black and red, Fig. 5b). This behaviour is unlike that of spin-coated 87PVA formulations, where spreading was a dominant mechanism (Fig. 2b). Instead, spreading behaviour becomes dominant after introducing glycerol to PVA of both DHs (blue and green for 87PVA and 99PVA, respectively, Fig. 5b).

Solution cast 87PVA films were very responsive to plasticisation, with *k* values increasing twice in magnitude for plasticised 87PVA compared to the non-plasticised counterpart. The magnitude of the

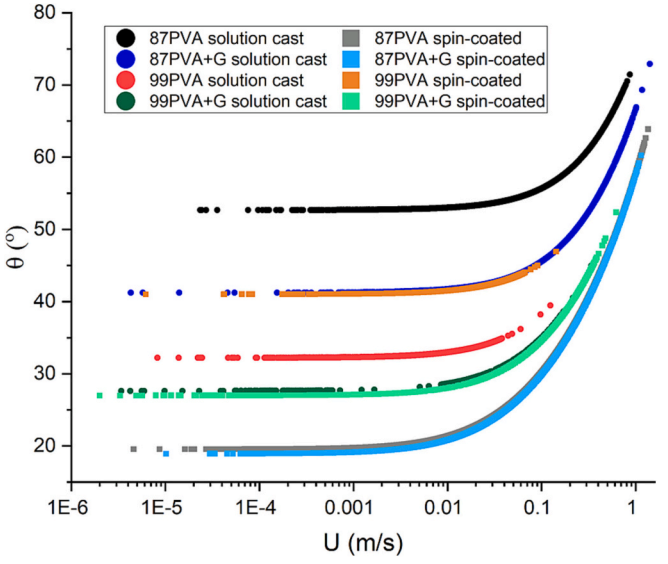

Fig. 4. Contact angle as a function of contact line velocity (*U*) for PVA-based formulations of various thickness and composition.

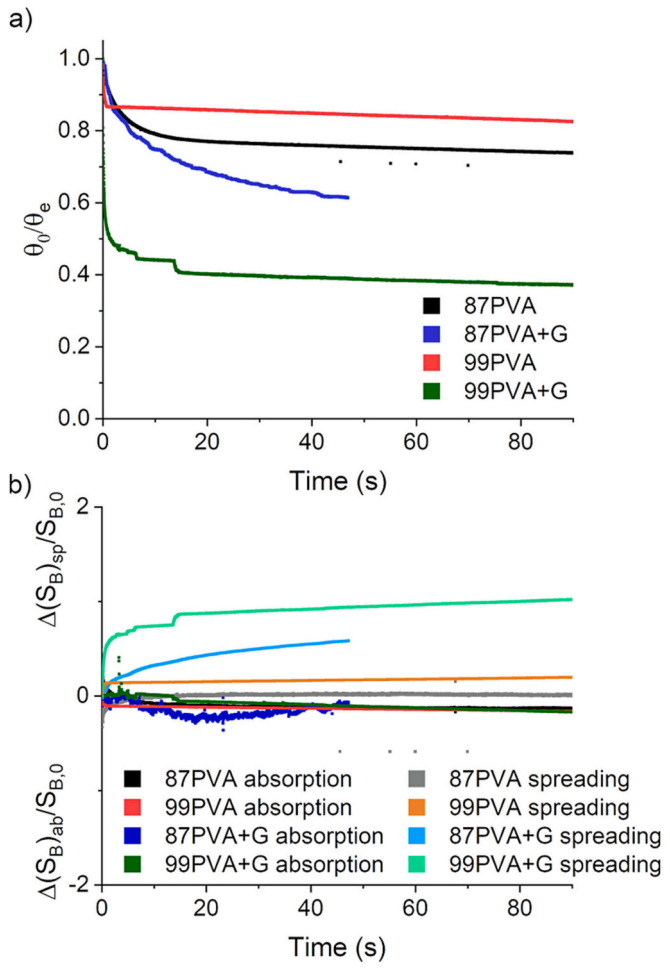

Fig. 5. (a) CA evolution for solution cast PVA-based films of various composition prepared from solutions of 10 % (w/v) concentration (400 µl), (b) Corresponding geometrical investigations (Eqs. (2)–(4)) for these samples. For interpretation of the references to colour in this figure, the reader is referred to the web version of this article.

fitted average time constant *k* decreased ca. 4× and 2× for 87PVA and plasticised 87PVA compared to the spin-coated counterparts, respectively, which corresponds to an overall slower water migration kinetics. For solution cast films of 99PVA (with and without glycerol), this trend was not observed, with the average *k* values remaining similar to their spin-coated equivalents (Fig. 3a, Table S2 in Supporting Information). Values of *n* for thin films were also greater compared to the solution cast formulations with the exception of 99PVA, where this trend is not as clear (Fig. 3b, Table S2 in Supporting Information), implying a lower propensity for spreading in solution cast films. Aside from plasticised 99PVA, the initial CA values for thick films were greater than for the thin films (Table 1). This can arise due to two reasons: first, polymer-substrate and polymer-air interactions can play an important role in the film behaviour for spin-coated formulations; second, differences in preparation method for the two film types could result in different matrix arrangement, including crystal structure more similar to the equilibrium one for solution cast polymer formulations compared to spin-coated ones.

The presence of an increased number of molecular layers in thick films also led to smaller ΔCA than in thin films with the notable exception of non-plasticised 99PVA which exhibited the same ΔCA in both film types (Table 1). In thick films, higher amount of water can infiltrate inside the film compared to thin counterparts, in general slowing down x,y-migration of water (on the surface) in favour of z-migration. Accordingly, ΔA values (change in drop surface area) were significantly lower for thick films than in thin films (again, aside from 99PVA, Table 1). Surprisingly, no significant difference in ΔV values was observed between the film preparation methods. These similar ΔV values imply a limitation in the goniometry technique itself: the strict geometrical assumptions used by the software to calculate droplet volume may lead to inaccuracies as the droplet becomes non-ideal upon absorption into the film. To account for this limitation and attempt to estimate ΔV indirectly, the discrepancy between measured droplet height and calculated droplet height assuming $\Delta V = 0$ was determined following Farris et al. [31] (not shown here, for brevity). This further analysis was inconclusive, therefore further study is required to determine if absorption phenomena are more prominent in thick films than thin films.

To summarise, CA evolution of water on PVA shows a clear distinction between PVA samples of different DH, as well as presence of plasticiser. Two possible underpinning mechanisms may cause this behaviour – polymer crystallinity and matrix tortuosity – and affect the rate of water ingress into the matrix.

3.5. FTIR characterisation of crystallinity in PVA-based formulations

FTIR was used to quantitatively evaluate the degree of crystallinity and characterise the PVA film by analysing the nature of hydroxyl and acetate groups, as well as interactions with any additives present. Detailed analysis of the spectra presented in Fig. 6 can be found in Supporting Information (Section S1 in Supporting Information).

Crystallinity of PVA film samples was estimated from the intensity ratio between peaks corresponding to crystalline phase at 1140 cm^{-1} (C—C stretching mode or C—O stretching) [37], and reference peaks: 850 cm^{-1} (CH_2 rocking) [36], 1425 cm^{-1} (CH_2 bending) [34,35], or 1094 cm^{-1} (C—O stretching) [34–38]. As FTIR is an indirect method to establish crystallinity in polymer films, the DC values were calculated using empirical formulas for crystallinity in the polymer films that utilise supplementary techniques such as XRD [38] or bulk density measurements [7] (Table 2).

It is worth noting that FTIR peaks corresponding to glycerol overlap with the 850, 1094, and 1141 cm^{-1} peaks used in DC calculations (Fig. 6). By comparing equivalent methods for plasticised and non-plasticised PVA, it becomes clear that the calculated DC is relatively higher in methods using these overlapping peaks (i.e. DC is reduced by ca. 20 % for the 1140/1425 peak ratio, but only by ca. 10 % for the 1140/850 and 1140/1094 peak ratio methods).

Overall, DC was approximately constant for all pure PVA samples, irrespective of film thickness or DH, but decreased upon introducing plasticiser to the mixture (Table 2). This suggests that observed changes in CA evolution behaviour are not exclusively correlated with the overall film crystallinity. Changes in CA evolution can be therefore explained in two possible ways: (i) small crystals, or those with low packing density, can be more readily dissolved [23] resulting in the exponential decay seen in Fig. 5a, while larger or more densely packed crystals (implying higher matrix tortuosity) lead to the linear CA evolution characteristic. Glycerol disrupts the hydrogen bonding network of the PVA, thus reducing DC and accelerating CA evolution [5]. Direct studies of crystallinity (e.g. using XRD) would be required to prove this hypothesis. (ii) While polymer crystallites create physical obstruction for water migration, they are embedded in PVA matrix of higher tortuosity for 99PVA formulations. Although DC and size might remain similar for the two types of PVA studied, decreased free volume in 99PVA films hinders water migration and has overriding effect on the overall behaviour.

3.6. Effect of aging RH conditions on the water spreading behaviour of thick films

Solution-cast thick PVA films were used to investigate the effect of RH on water CA evolution after 1 week of aging under 4 %, 45 %, and 100 % RH. As films were prepared in vacuum and investigated in

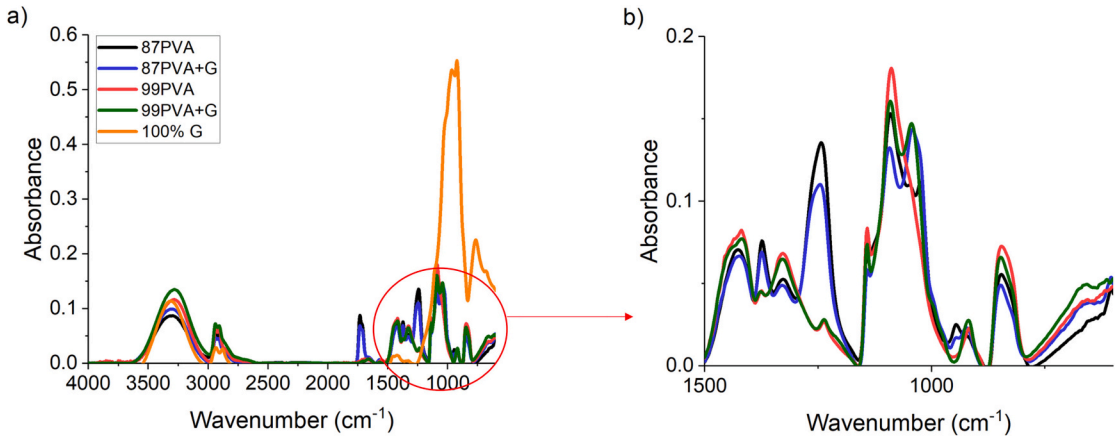

Fig. 6. FTIR spectra of PVA-based films of various composition prepared from solutions of 10 % (w/v) concentration (400 µl).

Table 2
Average DC values for all solution cast investigated compositions. Uncertainty values represent one standard deviation around the mean ($n = 5$).

Sample	Thickness (µm)	DC (1140/1425)	DC (Peppas et al.)	DC (1140/850)	DC (1140/1094)	DC (Tretinnikov et al.)
87PVA	30.6 ± 1.9	106.7 ± 0.4	45.8 ± 0.5	127.4 ± 0.4	47.2 ± 0.1	29.2 ± 0.1
	44.5 ± 3.8	104.6 ± 0.2	43.7 ± 0.2	135.2 ± 0.5	49.2 ± 0.1	30.9 ± 0.1
	87.0 ± 3.3	105.4 ± 0.3	44.6 ± 0.3	132.7 ± 0.8	48.4 ± 0.2	30.2 ± 0.2
	129.7 ± 7.6	105.3 ± 0.1	44.5 ± 0.1	137.6 ± 0.1	49.3 ± 0.1	31.0 ± 0.1
Plasticised 87PVA	21.7 ± 2.7	82.5 ± 0.2	21.1 ± 0.2	114.1 ± 0.2	42.5 ± 0.1	24.9 ± 0.1
	39.3 ± 5.5	76.8 ± 0.4	15.2 ± 0.5	107.2 ± 0.5	39.8 ± 0.2	22.5 ± 0.2
	73.5 ± 4.5	87.1 ± 0.3	25.8 ± 0.4	118.2 ± 0.3	43.9 ± 0.1	26.2 ± 0.1
	108.8 ± 3.0	87.4 ± 0.3	26.1 ± 0.4	118.3 ± 0.3	43.7 ± 0.13	26.0 ± 0.1
99PVA	52.8 ± 2.3	113.2 ± 0.4	52.5 ± 0.4	126.8 ± 0.4	49.5 ± 0.14	31.2 ± 0.1
	88.3 ± 4.6	110.9 ± 1.0	50.2 ± 1.1	123.6 ± 1.2	48.5 ± 0.32	30.3 ± 0.3
	129.7 ± 3.3	102.0 ± 0.1	41.0 ± 0.2	116.0 ± 0.2	46.5 ± 0.06	28.5 ± 0.1
	208.5 ± 2.2	103.9 ± 0.1	43.0 ± 0.1	118.2 ± 0.1	46.9 ± 0.03	28.9 ± 0.1
Plasticised 99PVA	33.1 ± 3.3	86.9 ± 0.2	25.5 ± 0.2	102.6 ± 0.3	41.6 ± 0.12	24.1 ± 0.1
	65.8 ± 3.0	86.8 ± 0.5	25.4 ± 0.5	104.1 ± 0.3	42.4 ± 0.15	24.8 ± 0.1
	119.8 ± 2.1	94.9 ± 0.3	33.7 ± 0.4	112.0 ± 0.1	45.9 ± 0.04	27.9 ± 0.1
	169.2 ± 4.1	95.4 ± 0.2	34.3 ± 0.2	112.9 ± 0.1	46.4 ± 0.05	28.4 ± 0.1

ambient RH (ca. 45 % RH), it is expected that the amount of water present in the sample would be higher than those equilibrated at 4 % RH, but below the counterpart stored at 45 % RH. Therefore, aging at conditions of high RH would result in plasticisation of the PVA matrix due to water vapour absorption, thereby accelerating CA progression.

After aging at low RH values (4 % and 45 % RH), no statistically significant changes in CA evolution were observed for 87PVA formulations compared to freshly-prepared equivalents (summarised in Fig. 7 and Tables S5, S6), however. The lack of changes observed with variable RH conditions were attributed to an insufficient aging of the samples, leading to only the surface layers of the matrix changing their molecular arrangement due to atmospheric water migration. This supposition is supported by further analysis - while T_g for both PVA matrices is expected to be above ambient temperature (ca. 70 °C for samples stored at low RH) [10,62], no change in contact line velocity as a function of CA (Eq. (6)) due to the polymer glass transition [60] was observed (not shown here, for brevity). Moreover, oscillations in the initial part of the CA evolution curves for all aged samples regardless of formulation (Fig. 8a, c), which were not observed for films investigated on day 0. Although the average the film behaviour was similar between freshly prepared samples and those aged at low humidity, individual measurements showed higher variability after aging (demonstrated in Fig. 7), with both linear (e.g. Fig. 8c, blue, red) and exponential CA evolution kinetics (e.g. Fig. 8c, black, maroon, and green) observed in plasticised 87PVA samples. While CA evolution showed primarily exponential character before aging, occasional measurements recorded the linear CA evolution profile (not shown here, for brevity), indicating that this behaviour results from the intrinsic properties of the films themselves (i.e. changes in molecular packing, intermolecular interactions between polymer chains and water within droplet area as a result of water migration during film storage). Upon aging, however, linear CA evolution was observed more frequently, resulting in changes in averaged k and n parameters compared to freshly prepared samples (Figs. 3 and 7). For 99PVA films (both plasticised and non-plasticised), variability in CA evolution did not increase upon aging, however aging at both 45 % RH and 4 % RH caused slower CA evolution rates compared to formulations investigated on day 0. For 99PVA films (both plasticised and non-plasticised), aging at these humidity values had a similarly minor effect, showing slightly slower CA evolution rates compared to formulations investigated on day 0.

These changes in CA evolution can be correlated with changes in molecular arrangement due to water and glycerol migration in the PVA matrix: reorientation of the polymer chain ends so that the hydrophobic parts are exposed at the air-film interface, resulting in differences in wetting kinetics [40]. 87PVA is more sensitive to these changes due to the overall lower amount of -OH groups available compared to 99PVA films and lower M_w (hence quicker reorientation). Changes in other parameters (ΔCA, initial CA values, ΔA, ΔV, Table 1 and Tables S8–S10 in Supporting Information) do not show clear differences between freshly prepared and aged films. As below ca. 30 wt%, water is only present in the PVA film in a nonfreezing state, the absolute humidity is not enough to cause significant changes in matrix properties for investigated thickness of the film. While 45 % and lower RH values are sufficient to cause molecular migration of the surfactant for thin films [68], thickness of the films (and ratio of the surface water layer to the film thickness) likely determines the minimum absolute humidity for these

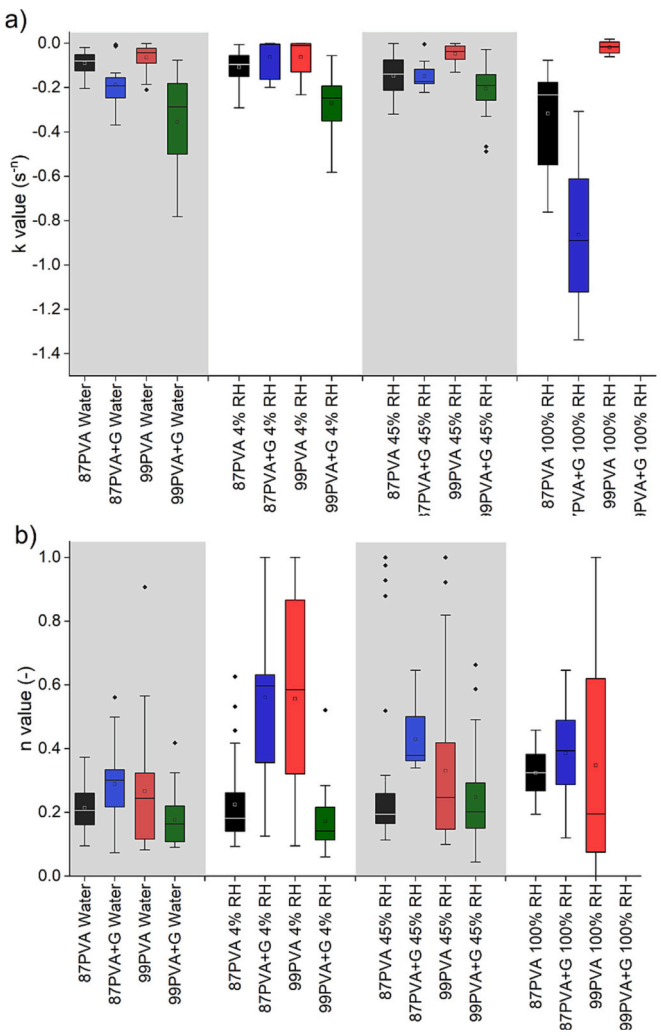

Fig. 7. Box and whisker graphs of Farris model (Eq. (1)) fits for parameter (a) *k* and (b) *n* for spreading of water on samples stored at various RH conditions.

effects to be observed. Not reaching the threshold of maximum nonfreezing water content therefore provides a good explanation for the similar behaviour of 4 wt% and 45 % RH in this work.

The most significant changes in wetting kinetics were noted for samples stored under 100 % RH condition, whereby PVA films visibly shown morphological changes as the result of absorbing water from the atmosphere. 87PVA samples formed a gel-like structure that attached to the supporting substrate while 99PVA samples became a swollen film that no longer adhered to the substrate. CA measurements were not practically possible on the majority of the plasticised and non-plasticised PVA films due the uneven surfaces, rendering image analysis infeasible. From the measurements that were possible, it can be concluded that aging at 100 % RH would result in instantaneous infiltration of the water droplet into the PVA film (ca. 2× and 4× decrease in magnitude of parameter *k* for non-plasticised and plasticised 87PVA, respectively, Fig. 7a, Table S7 in Supporting Information), as PVA-based films are above their T_g (−14 °C for storage at 86 % RH) [62].

These observations were further confirmed by crystallinity measurements. No clear trend or substantial changes in FTIR spectra was observed for samples stored at 4 % RH and 45 % RH in comparison to the freshly prepared ones (Fig. 9). It is concluded that no variations in intermolecular interactions or DC took place because environmental aging only affects the surface layer of the film (while ATR-FTIR crystal penetration depth is equal to ca. 2 μm). Among the few notable observations, there is an increased ratio of 3300/2900 peak (OH stretching correlated with hydrogen bonds/CH_2 stretching and bending) [34,37,63,64] for 99PVA samples stored at 4 % RH: peaks were found to shift slightly to lower wavenumbers, which indicate small variations in the characteristics of hydrogen bonding in the system. Overall, FTIR results indicate that DC was not significantly changed over time at ambient RH – neither in terms of further crystallisation nor crystallite dissolution.

For samples stored at 100 % RH, no conclusions about crystallinity changes can be drawn for 87PVA-based samples due to clear changes in the matrix structure and consequent non-physical DC values obtained. For these formulations, characteristic PVA peaks were no longer visible, being replaced by peaks at 900 and 1000 cm^{-1} with an increased absorbance of hydrogen bond peak at 3300 cm^{-1}. Hence, a modified water spectrum was observed rather than polymer spectrum. For 99PVA-based films, however, FTIR measurements were possible, showing clearly decreased DC after storage at 100 % RH. Plasticised films showed more significant decrease in DC compared to samples investigated on day 0 calculated according to the Peppas model [7] based on 1140/1425 peak ratio (41 % and 57 % decrease for non-plasticised and plasticised films, respectively, Table 2 and S4 in Supporting Information), compared to other two methods: a 10 % and 21 % decrease for non-plasticised and plasticised films, respectively, for crystallinity defined as ratio of 1140/850 cm^{-1} peaks; and 17 % and 31 % decrease for non-plasticised and plasticised films, respectively, for crystallinity defined according to the Trettinikov model (based on 1150/1094 peaks) [38]. While water content increased in the polymer matrix, the most significant changes in the structure were associated with hydrogen bonding and C-OH group interactions (950 cm^{-1}). Accordingly, an individual peak at 1050 cm^{-1} was no longer visible, indicating overall weaker C—O stretching interactions, with increased importance of hydrogen bonding observed again as water ingress replaced PVA-PVA hydrogen bonds with PVA-water hydrogen bonds [20]. This resulted in creation of liquid-like clusters for samples stored at 100 % RH that further changed the character of intermolecular interactions in polymer systems [20].

To interpret the findings of water migration on PVA films, one must consider the thermodynamics of polymer dissolution. Water uptake in polymer films is controlled by solvation of the polymer chains [24] as dissolution involves two processes: solvent diffusion and chain disentanglement that changes polymer from glassy to rubbery state [65]. Dissolution occurs in layers: first by solvent filling the matrix free volume; then the amorphous, glassy polymer matrix will undergo transition into gel-like swollen layer due to diffusion of the solvent into the film (as can be observed in samples aged at 100 % RH). Consequently, two separate interfaces are formed: between glassy polymer and gel layer, and between gel layer and the solvent. After an induction time, polymer dissolution takes place [65].

According to Uerberreiter [65], dissolution of polymer films results in formation of multiple layers: pure polymer, infiltration layer, solid swollen layer, gel layer, liquid layer and pure solvent. The polymer dissolves into surrounding solvent, while solvent migrates into polymer matrix creating more rubber-like polymer structure. Water concentration gradient within the matrix is the driving force for further changes in the layers below those in direct contact with the solvent. Therefore, solvent penetration into the polymer results in an increased thickness of swollen surface until this process becomes polymer diffusion controlled [65]. In the presented study, the water in contact with the PVA film was found in a surface adsorbed layer, determined by the vapour-liquid equilibrium at the film surface [66]. Despite this lack of pure solvent phase, the difference in aging behaviour as a function of polymer DH (which follows trends in bulk solubility of the corresponding polymer) proves that this model is at least partially valid for describing the aging of polymer films at 100 % RH.

The nature of the polymer chain itself determines much of the internal film structure and hence its ease of dissolution when in contact with water. For uncrosslinked, amorphous polymers, differences in free

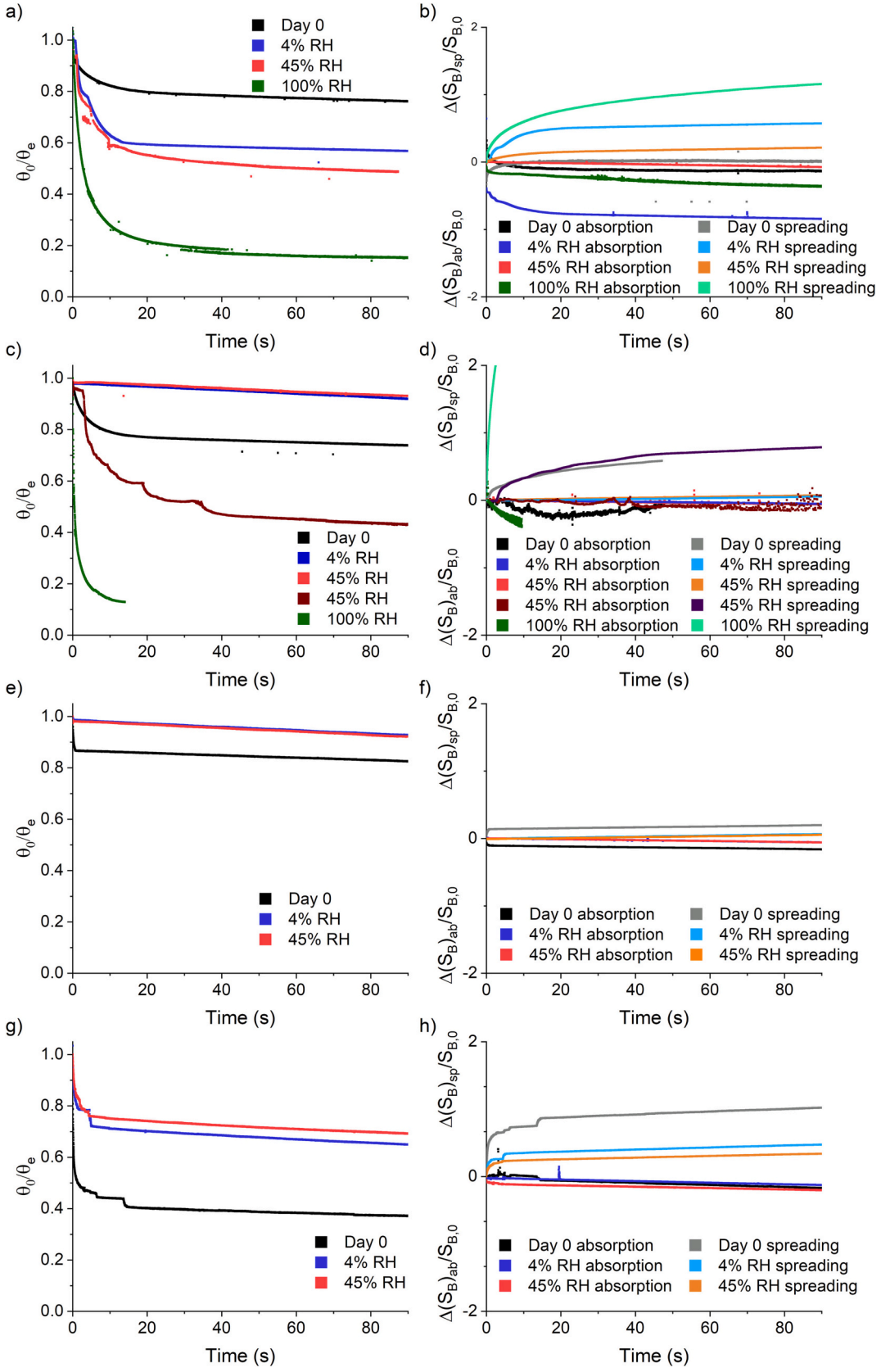

Fig. 8. CA evolution with time and corresponding geometrical investigations for solution cast films: (a, b) 87PVA, (c, d) plasticised 87PVA, (e, f) 99PVA, (g, h) plasticised 99PVA. For interpretation of the references to colour in this figure, the reader is referred to the web version of this article.

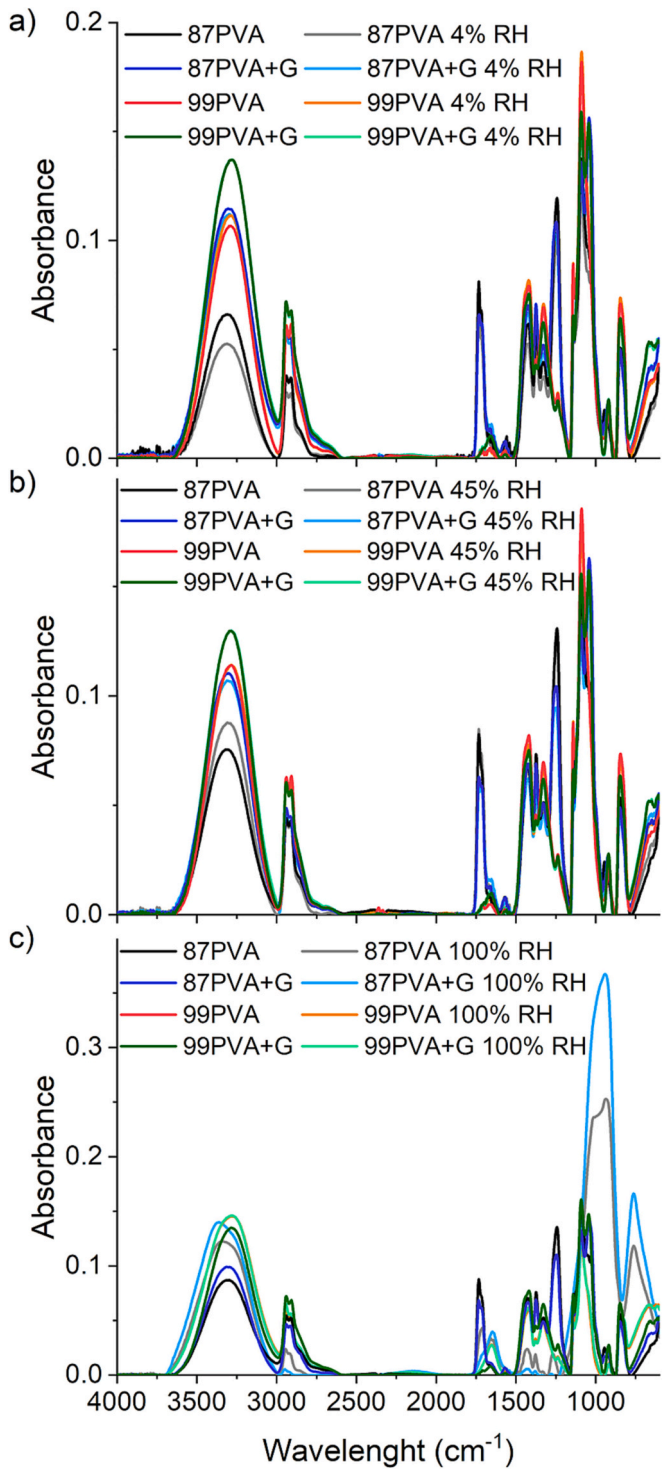

Fig. 9. FTIR spectra of solution cast PVA-based films stored at various RH conditions, compared against freshly prepared samples. (a) 4 % RH (ambient RH), (b) 45 % RH, and (c) 100 % RH.

volume and segmental stiffness, along with the tacticity of the polymer [65], determine their dissolution rate. Despite its overall atactic configuration, PVA has high preference to create crystallites because of the relatively small size of the hydroxyl group and strength of hydrogen bonding [20]. Water can be bonded to the polymer on one side (weak bonding), two sides (strong bonding) and be placed in the interface region between crystallites and amorphous region of the polymer [20]. Changes in polymer dissolution behaviour are therefore a direct consequence of physical crosslinks (crystallites) present in the system which act to slow migration rates compared to completely amorphous matrices. Moreover, the dissolution rate was proven to be inversely proportional to the polymer M_w up to a certain limit characteristic for a given polymer [65]. This is connected with the chain disentanglement that is a function of a polymer M_w - generally, the higher the M_w, the higher the level of disentanglement required before swelling and dissolution can occur [65,67].

The high M_w and increased number of -OH groups (available sites to form hydrogen bond with infiltrating water molecules) in the 99PVA polymer result in overall more compact molecular packing, which is less influenced by the infiltrating water than 87PVA samples. From the similar behaviour of plasticised versus non-plasticised formulations after swelling, one can conclude that the increased chain entanglement is the primary reason for these contrasts between different DH values. Moreover, changes in the morphology of the crystallites are believed to be the consequence of differences between 87PVA and 99PVA formulations. While addition of glycerol influences the matrix crystallinity, it does not change the continuity of 99PVA film upon water infiltration. According to the description by Uerberreiter, the 99PVA film as a whole behaves like a swollen polymer layer, while the 87PVA film behaves as a gel.

4. Conclusions

The dissolution behaviour of water-soluble PVA films was investigated using CA goniometry. We observed that the kinetics of CA evolution is determined by film composition - primarily DH and M_w of the polymer, presence of glycerol in the system, and the film preparation method (spin coating vs solution casting). Both thin and thick films prepared with partially hydrolysed PVA showed a longer initial period of CA evolution with overall higher change (exponential trend), followed by slower, linear change of CA when compared against fully hydrolysed PVA.

For 99PVA formulations, this initial period of significant changes was short, and followed by a linear decrease in CA, resulting in a significantly slower overall CA changes compared to 87PVA film. We suggest that size and morphology of the crystallites (despite non-significant changes in overall DC between these samples), higher M_w for 99PVA film compared to 87PVA film (resulting in higher level of chain entanglement), changes in polymer structure (amount of -OH groups), and differences in free volume within the matrix are all responsible for the difference observed. These changes are not correlated with film thickness, however, as evidenced by no substantial changes with film thickness for the samples prepared in the same way. Instead, different wetting behaviour appears for thin films compared to thick films – fast spreading on the surface and overall low ΔCA that can be approximated as wetting taking place only in the x,y-dimension.

Introducing glycerol to PVA matrix leads to plasticisation of polymer chains and results in drastic changes of CA, with spreading playing a more significant role compared to non-plasticised samples. It is suggested that plasticisation has a more global effect in 87PVA (increase in free volume and flexibility of the chains) compared to 99PVA. Possible changes in crystallite structure upon glycerol addition or changes in liquid surface tension as the polymer solvates result in step-like changes in CA for the latter polymer.

Aging PVA samples at 4 % and 45 % RH did not result in significant changes in either CA evolution or in FTIR spectrum, although droplet instabilities were observed at the beginning of the process. This is likely due to an insufficient water infiltration into the PVA film from the atmosphere to exceed the threshold of nonfreezing water in the system or variations in the glycerol local concentration. For 100 % RH, the initial stages of PVA dissolution as a consequence of water absorption were observed, with measurements being impossible to perform due to non-uniformities of the surface. Changes in the DH and polymer matrix packing are believed to be the reason for swollen polymer and gel-like

behaviour for 99PVA and 87PVA-based formulations, respectively. These findings provide initial insight into the mechanism of product failure because of the environmental conditions during storage, although longer timescales might be required to expand understanding to the full product lifecycle.

Declaration of competing interest

The authors declare that they have no known competing financial interests or personal relationships that could have appeared to influence the work reported in this paper.

Data availability

Data will be made available on request.

Acknowledgements

This research was funded by School of Chemical Engineering, University of Birmingham, and Engineering & Physical Science Research Council (EPSRC) with grant number EP/P007864/1. ZJZ acknowledges an Industrial Fellowship with P&G, funded by the Royal Academy of Engineering (IF2021\100).

Appendix A. Supplementary data

Supplementary data to this article can be found online at https://doi.org/10.1016/j.porgcoat.2023.107436.

References

[1] I.C.F. Moraes, R.A. Carvalho, A.M.Q.B. Bittante, J. Solorza-Feria, P.J.A. Sobral, Film forming solutions based on gelatin and Poly(Vinyl Alcohol) blends: thermal and rheological characterizations, J. Food Eng. 95 (4) (2009) 588–596.
[2] A. Hasimi, A. Stavropoulou, K.G. Papadokostaki, M. Sanopoulou, Transport of water in polyvinyl alcohol films: effect of thermal treatment and chemical crosslinking, Eur. Polym. J. 44 (12) (2008) 4114–4123.
[3] C. DeMerlis, D. Schoneker, Review of the Oral toxicity of polyvinyl alcohol (PVA), Food Chem. Toxicol. 41 (3) (2003) 319–326.
[4] Hassan, C. M.; Trakampan, P.; Peppas, N. A. Water Solubility Characteristics of Poly(Vinyl Alcohol) and Gels Prepared by Freezing/Thawing Processes. In Water Soluble Polymers; Kluwer Academic Publishers: Boston; pp 31–40.
[5] L.Y. Lim, L.S.C. Wan, The effect of plasticizers on the properties of polyvinyl alcohol films, Drug Dev. Ind. Pharm. 20 (6) (1994) 1007–1020.
[6] A.A. Aydın, V. Ilberg, Effect of different polyol-based plasticizers on thermal properties of polyvinyl alcohol: starch blends, Carbohydr. Polym. 136 (2016) 441–448.
[7] N. Peppas, Infrared spectroscopy of semicrystalline Poly(Vinyl Alcohol) networks, Die Makromol. Chem. 178 (2) (1977) 595–601.
[8] A. Briddick, R.J. Fong, E.F.D. Sabattié, P. Li, M.W.A. Skoda, F. Courchay, R. L. Thompson, Blooming of smectic Surfactant/Plasticizer layers on spin-cast Poly (Vinyl Alcohol) films, Langmuir 34 (4) (2018) 1410–1418.
[9] M. Mohsin, A. Hossin, Y. Haik, Thermal and mechanical properties of Poly(Vinyl Alcohol) plasticized with glycerol, J. Appl. Polym. Sci. 122 (5) (2011) 3102–3109.
[10] R.J. Fong, A. Robertson, P.E. Mallon, R.L. Thompson, The impact of plasticizer and degree of hydrolysis on free volume of Poly(Vinyl Alcohol) films, Polymers (Basel). 10 (9) (2018) 1036.
[11] A.P. Verrall, P.S. Bening, K.A. Kugler, Polyvinyl Alcohol Complymer Film for Packaging Liquid Products and Having an Improved Shelf-Life, 2010.
[12] P. Bergo, I.C.F. Moraes, P.J.A. Sobral, Effects of different moisture contents on physical properties of PVA-gelatin films, Food Biophys. 7 (4) (2012) 354–361.
[13] R.M. Hodge, T.J. Bastow, G.H. Edward, G.P. Simon, A.J. Hill, Free volume and the mechanism of plasticization in water-swollen Poly(Vinyl Alcohol), Macromolecules 29 (25) (1996) 8137–8143.
[14] R.M. Hodge, G.H. Edward, G.P. Simon, Water absorption and states of water in semicrystalline Poly(Vinyl Alcohol) films, Polymer (Guildf). 37 (8) (1996) 1371–1376.
[15] W.Z. Zhang, M. Satoh, J. Komiyama, A differential scanning calorimetry study of the states of water in swollen Poly(Vinyl Alcohol) membranes containing nonvolatile additives, J. Membr. Sci. 42 (3) (1989) 303–314.
[16] Z. Waheed, Y. Dong, N. Han, S. Liu, Water and gas barrier properties of polyvinyl alcohol (PVA)/ starch (ST)/ glycerol (GL)/ halloysite nanotube (HNT) bionanocomposite films : experimental characterisation and modelling approach, Compos. Part B 174 (February) (2019), 107033.
[17] M. Asem, W.M.F.W. Nawawi, D.N. Jimat, Evaluation of water absorption of polyvinyl alcohol-starch biocomposite reinforced with sugarcane bagasse nanofibre: optimization using two-level factorial design, IOP Conf. Ser. Mater. Sci. Eng. 368 (2018), 012005.
[18] M. Lim, D. Kim, H. Han, S.B. Khan, J. Seo, Water sorption and water-resistance properties of Poly(Vinyl Alcohol)/Clay nanocomposite films: effects of chemical structure and morphology, Polym. Compos. 36 (4) (2015) 660–667.
[19] F.A. Long, L.J. Thompson, Diffusion of water vapor in polymers, J. Polym. Sci. 15 (80) (1955) 413–426.
[20] P.S. Thomas, B.H. Stuart, A fourier transform raman spectroscopy study of water sorption by Poly(Vinyl Alcohol), Spectrochim. Acta Part A Mol. Biomol. Spectrosc. 53 (13) (1997) 2275–2278.
[21] G.S. Kulagina, A.E. Chalykh, V.K. Gerasimov, K.A. Chalykh, T.P. Puryaeva, Sorption of water by poly(vinyl alcohol), Polym. Sci. Ser. A 49 (4) (2007) 425–432.
[22] E.El Shafee, H.F. Naguib, in: Water Sorption in Cross-linked Poly (Vinyl Alcohol) Networks 44, 2003, pp. 1647–1653.
[23] T. Tanigami, K. Yano, K. Yamaura, S. Matsuzawa, Anomalous swelling of Poly (Vinyl Alcohol) film in mixed solvents of dimethylsulfoxide and water, Polymer (Guildf). 36 (15) (1995) 2941–2946.
[24] L.M. Döppers, C. Breen, C. Sammon, Diffusion of water and acetone into Poly(Vinyl Alcohol)-clay nanocomposites using ATR-FTIR, Vib. Spectrosc. 35 (1–2) (2004) 27–32.
[25] S.Q. Shi, D.J. Gardner, Dynamic adhesive wettability of wood, Wood Fiber Sci. 33 (1) (2001) 58–68.
[26] T. Liu, J. Hao, B. Yang, B. Hu, Z. Cui, S. Li, Contact angle measurements: an alternative approach towards understanding the mechanism of increased drug dissolution from ethylcellulose tablets containing surfactant and exploring the relationship between their contact angles and dissolution behaviors, AAPS PharmSciTech 19 (4) (2018) 1582–1591.
[27] M.E.R. Shanahan, C. Bourgès, Effects of evaporation on contact angles on polymer surfaces, Int. J. Adhes. Adhes. 14 (3) (1994) 201–205.
[28] Z. Zhang, M. Moxey, A. Alswieleh, A.J. Morse, A.L. Lewis, M. Geoghegan, G. J. Leggett, Effect of salt on phosphorylcholine-based zwitterionic polymer brushes, Langmuir 32 (20) (2016) 5048–5057.
[29] A. Marmur, Advances in Colloid and Interface Science 19 (1983) 75–102.
[30] V. Dutschk, K.G. Sabbatovskiy, M. Stolz, K. Grundke, V.M. Rudoy, in: Unusual Wetting Dynamics of Aqueous Surfactant Solutions on Polymer Surfaces 267, 2003, pp. 456–462.
[31] S. Farris, L. Introzzi, P. Biagioni, T. Holz, A. Schiraldi, L. Piergiovanni, Wetting of biopolymer coatings: contact angle kinetics and image analysis investigation, Langmuir 27 (12) (2011) 7563–7574.
[32] Y.F. Lin, T.I. Yeh, K.H. Chan, T.S. Chen, The automatic calibration system of humidity fixed points at CMS, Measurement 19 (2) (1996) 65–71.
[33] Z.M. Zhang, S. Chen, Y.Z. Liang, Baseline correction using adaptive iteratively reweighted penalized least squares, Analyst 135 (5) (2010) 1138–1146.
[34] N.V. Bhat, M.M. Nate, M.B. Kurup, V.A. Bambole, S. Sabharwal, Effect of γ-radiation on the structure and morphology of polyvinyl alcohol films, Nucl. Inst. Methods Phys. Res. B 237 (3–4) (2005) 585–592.
[35] S.J. Lue, J.Y. Chen, J.M. Yang, Crystallinity and stability of poly(vinyl alcohol)-fumed silica mixed matrix membranes, J. Macromol. Sci. Part B Phys. 47 (1) (2008) 39–51.
[36] J. Lee, K. Jin Lee, J. Jang, Effect of silica nanofillers on isothermal crystallization of Poly(Vinyl Alcohol): in-situ ATR-FTIR study, Polym. Test. 27 (3) (2008) 360–367.
[37] H.S. Mansur, C.M. Sadahira, A.N. Souza, A.A.P. Mansur, FTIR spectroscopy characterization of poly (Vinyl Alcohol) hydrogel with different hydrolysis degree and chemically crosslinked with glutaraldehyde, Mater. Sci. Eng. C 28 (4) (2008) 539–548.
[38] O.N. Tretinnikov, S.A. Zagorskaya, Determination of the degree of crystallinity of Poly(Vinyl Alcohol) by FTIR spectroscopy, J. Appl. Spectrosc. 79 (4) (2012) 521–526.
[39] C. Ton-That, A.G. Shard, R.H. Bradley, Thickness of spin-cast polymer thin films determined by angle-resolved XPS and AFM tip-scratch methods, Langmuir 16 (5) (2000) 2281–2284.
[40] F. Lequeux, L. Talini, E. Verneuil, G. Delannoy, P. Valois, Wetting of polymers by their solvents, Eur. Phys. J. E 39 (2) (2016) 12.
[41] A. Marangoni, Fat Crystal Networks; New York, 2005.
[42] D. Muscat, R.A.L. Drew, Modeling the infiltration kinetics of molten aluminum into porous titanium carbide, Metall. Mater. Trans. A 25 (11) (1994) 2357–2370.
[43] S. Newman, Kinetics of wetting of surfaces by polymers; capillary flow, J. Colloid Interface Sci. 26 (2) (1968) 209–213.
[44] T.D. Blake, A. Clarke, in: Contact Angle Relaxation During Droplet Spreading 121, 1997, pp. 2164–2166, 11.
[45] T.P. Yin, The kinetics of spreading, J. Phys. Chem. 73 (7) (1969) 2413–2417.
[46] N.M. Kovalchuk, A. Trybala, O. Arjmandi-tash, V. Starov, Surfactant-enhanced spreading : experimental achievements and possible mechanisms, Adv. Colloid Interf. Sci. 233 (2016) 155–160.
[47] H.Van Oene, Y.F. Chang, S. Newman, The rheology of wetting by polymer melts, J. Adhes. 1 (1) (1969) 54–68.
[48] M.D. Lelah, A. Marmur, Spreading kinetics of drops on glass, J. Colloid Interface Sci. 82 (2) (1981) 518–525.
[49] B.W. Cherry, C.M. Holmes, Kinetics of wetting of surfaces by polymers, J. Colloid Interface Sci. 29 (1) (1969) 174–176.
[50] H. Schonhorn, H.L. Frisch, T.K. Kwei, Kinetics of wetting of surfaces by polymer melts, J. Appl. Phys. 37 (13) (1966) 4967–4973.
[51] P.G. de Gennes, Wetting: statics and dynamics, Rev. Mod. Phys. 57 (3) (1985) 827–863.

[52] P. Muralidhar, E. Bonaccurso, G.K. Auernhammer, H.J. Butt, Fast dynamic wetting of polymer surfaces by miscible and immiscible liquids, Colloid Polym. Sci. 289 (14) (2011) 1609–1615.
[53] Litwinowicz, M. A.; Rogers, S.; Tellam, J.; Thompson, R. L. Tuning the Bulk and Surface Properties of PDMS Networks through Cross-Linker and Surfactant Concentration. Prep.
[54] R.J. Fong, A. Robertson, P.E. Mallon, R.L. Thompson, Polymers the impact of plasticizer and degree of hydrolysis on free volume of poly (vinyl alcohol), Films (2018) 1–15.
[55] A. Briddick, Exploring Surfactant and Plasticiser Segregation in Thin PVA Films, University of Durham, 2017.
[56] A.-J. Li, R. Nussinov, A set of van Der waals and coulombic radii of protein atoms for molecular and solvent-accessible surface calculation, packing evaluation, and docking, Proteins Struct. Funct. Genet. 32 (1) (1998) 111–127.
[58] J. Jang, D.K. Lee, Plasticizer effect on the melting and crystallization behavior of polyvinyl alcohol, Polymer (Guildf). 44 (26) (2003) 8139–8146.
[59] A. Camós Noguer, S.M. Olsen, S. Hvilsted, S. Kiil, Diffusion of surface-active amphiphiles in silicone-based fouling-release coatings, Prog. Org. Coat. 106 (2017) 77–86.
[60] J. Dupas, E. Verneuil, M. Van Landeghem, B. Bresson, L. Forny, M. Ramaioli, F. Lequeux, L. Talini, Glass transition accelerates the spreading of polar solvents on a soluble polymer, Phys. Rev. Lett. 112 (18) (2014), 188302.
[62] M.V. Konidari, K.G. Papadokostaki, M. Sanopoulou, Moisture-induced effects on the tensile mechanical properties and glass-transition temperature of Poly(Vinyl Alcohol) films, J. Appl. Polym. Sci. 120 (6) (2011) 3381–3386.
[63] N.M. El-Sawy, M.B. El-Arnaouty, A.M. Abdel Ghaffar, Γ-irradiation effect on the non-cross-linked and cross-linked polyvinyl alcohol films, Polym. Plast. Technol. Eng. 49 (2) (2010) 169–177.
[64] S. Hadad, S.A.H. Goli, Fabrication and characterization of electrospun nanofibers using flaxseed (Linum Usitatissimum) mucilage, Int. J. Biol. Macromol. 114 (2018) 408–414.
[65] B.A. Miller-Chou, J.L. Koenig, A review of polymer dissolution, Prog. Polym. Sci. 28 (8) (2003) 1223–1270.
[66] K.S. Lee, N. Ivanova, V.M. Starov, N. Hilal, V. Dutschk, Kinetics of wetting and spreading by aqueous surfactant solutions, Adv. Colloid Interf. Sci. 144 (1–2) (2008) 54–65.
[67] E.E. Parsonage, Properties of positive resists. II. Dissolution characteristics of irradiated poly(methyl methacrylate) and poly(methyl methacrylate–co-maleic anhydride), J. Vac. Sci. Technol. B Microelectron. Nanom. Struct. 5 (2) (1987) 538.
[68] Majerczak, K.; Shi, Z.; Zhang, Z.; Zhang, Z. Humidity- and Surfactant-Accelerated Aging of Molecular Thin Films. Prep.